Lotus effect on Al-surfaces

D. K. Sarkar and M. Farzaneh

Canada Research Chair on Atmospheric Icing Engineering of Power Networks (INGIVRE) and Industrial Chair on Atmospheric Icing of Power Network Equipment (CIGELE), 555 Boul. de l' Université, Université du Québec à Chicoutimi, Canada G7H 2B1

ABSTRACT

Nanostructured patterns have been produced on aluminum surfaces by chemical etching. The density of these nanopatterns increases with an increase in concentration of the etchant. The patterned aluminum surfaces have been passivated using stearic acid (SA) organic molecules. The passivated surfaces are found to be superhydrophobic exhibiting the lotus effect. The contact angle of water on these surfaces is found to increase initially with the increase of deposition time of stearic acid and saturate afterwards. The hydrophilic tails of SA molecules interact with the aluminum surfaces keeping the hydrophobic heads upwards. The contact angle of water on these surfaces have been found to be as high as 170^o with a contact angle hysteresis as low as 4^o. The formation of nanopatterns on micrograins of aluminum and the presence of upward hydrophobic heads of SA molecules lead to the lotus effect on aluminum surfaces.

Keywords: Lotus effect, Superhydrophobic, Chemical etching

1 INTRODUCTION

Nature is the best inspiring example for superhydrophobicity in various botanical and zoological objects including more than 200 plants such as iris, lotus, tulipa etc. and in creatures such as the water-strider, the butterfly, etc. [1-4]. This extraordinary property that aids in self-cleaning is popularly known as Lotus Effect, lets water drops rolls off their surfaces taking the dirt away [1, 5]. Inspired by nature, there have been several efforts to mimic such surfaces on a desired substrate [6-10]. Such a surface, which exhibits a very high contact angle of water and a very low contact angle hysteresis, lets water drops roll off even with the slightest inclination and thus has tremendous potential applications in various areas such as in microfluidic devices, textile industries and anti-icing materials. Various techniques used to fabricate such surfaces include lithography [6], sol-gel [7], plasma etching [8,9], chemical etching [10] etc. Recently, chemical etching has been used to achieve superhydrophobicity on copper surfaces by passivating them using fluoroalkylsilane (FAS) organic molecules with $-CF_3$ terminated radicals [10].

In this paper we discuss the creation of a binary structure containing micro-nanosteps very similar to the structure observed in lotus leaves. Aluminum is of a particular interest due to its versatile application in heavy industries (electrical cables, aircrafts, etc) as well as in Microelectromechanical systems (MEMS) devices. The results of the evolution of the nanostructure formation and superhydrophobicity of these nanostructure surfaces with respect to passivation using $-CH_3$ terminated organic molecules will be discussed.

2 EXPERIMENTAL

Aluminum surfaces were etched using 37% *HCl* solution diluted with deionized water. The volume ratio of $HCl:H_2O$ was chosen as 60:40, 50:50, 40:60, 30:70 and 20:80. The etching time was chosen to be longer for lower concentrated acid solution. All the etched samples were ultrasonically cleaned with deionized water to remove any residual dust particles from the pores of the nanosurface. The cleaned samples were dried at 70 ^{o}C for more than 10 hours and then passivated both by spin-coating and by dipping them for more than 30 minutes in a solution prepared by dissolving 2×10^{-3} molar stearic acid (SA) in acetone. A few silicon samples were passivated in the same manner for Fourier Transform Infrared Spectroscopy (FTIR) investigation. The passivated samples were dried at 70 ^{o}C for more than 2 hours. The surface morphology of the samples were investigated using LEO field emission scanning electron microscopy (FESEM) and Nanoscope IIIa Digital instrument Atomic force microscopy (AFM). The FTIR investigations of the passivated samples were carried out using a PerkinElmer Spectrum One FT-IR spectrometer in the wavenumber range of 400-4000 cm^{-1}. Equilibrium contact angle (CA) measurements were made using a Krüss DSA100 goniometer. The volume of water drop used for the CA measurements was 6 μL of deionized water that was dropped onto the sample by use of a hydrophobized needle attached to a micro-syringe. A picture of the water drop was taken a few seconds after dropping it to avoid any error related to its evaporation. Tangent measurements were made on the profile of the drops, and several images were taken to obtain the average of the contact angle.

3 RESULTS AND DISCUSSION

Figure 1(a) shows a FESEM micrograph of Al surface etched with 30% HCl solution ($HCl:H_2O$=30:70 by volume)

and Figure 1(b) shows the same with 40 % HCl solution ($HCl:H_2O$=40:60 by volume). The samples that have been etched with 30% and 40% acid solution will be called Al30 and Al40, respectively.

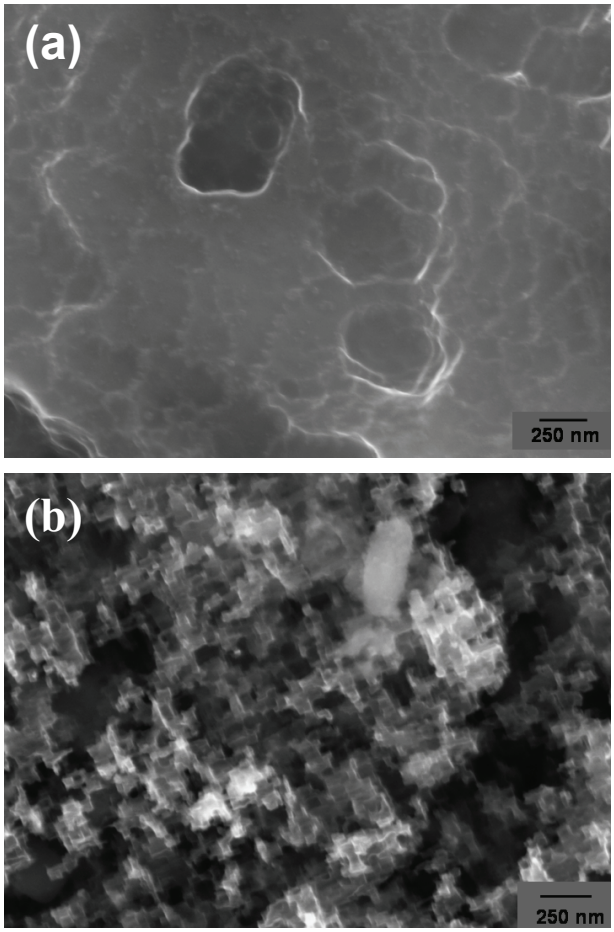

Figure 1 FESEM images of (a) Al30 and (b) Al40.

The Al30 sample was etched for 20 minutes and the Al40 one for only 5 minutes. It is evident from the images that the number of etch pits increases with the increase in the concentration of the acid. In a crystalline metal, there exist a large number of dislocation defects. Due to their high energy, these defect sites are easily attacked by the chemical etchant and get dissolved first as compared to defect-free parts of a crystal [11]. The etch pit formation occurs due to the preferential nucleation of one atom-deep-single pits at a dislocation site and the movement of the monatomic steps across the surface. The shape of an etch pit depends on the growth rate of these two processes. The dissolution rates normal to the surface (V_n) and parallel to the surface (V_s) at a dislocation determine the shape of an etch pit. Deeper etch can be obtained if V_n is larger than V_s. In addition, the creation of etch pits is a statistical process and depends on the concentration of the acid. A larger number of etch pits are likely to be created with higher concentration of etchant. As expected, more etch pit formations were observed on the Al40 surface than on the Al30 surface by increasing the concentration of the solution by only 10%. Also, it was noticed that increasing the etching time causes the depth of the etched pits to increase (Figure is not shown). Figure 2 shows the AFM image and the section analysis of sample Al40 with a scan size of 2 μm×2 μm. It is clear from the section analysis of the AFM that each micropattern consists of several nanosteps which effectively increases the overall surface area on aluminum sample, as found in the lotus leaf with a similar microstructure. The steps are nearly 100 nm and 30 nm high as investigated by AFM.

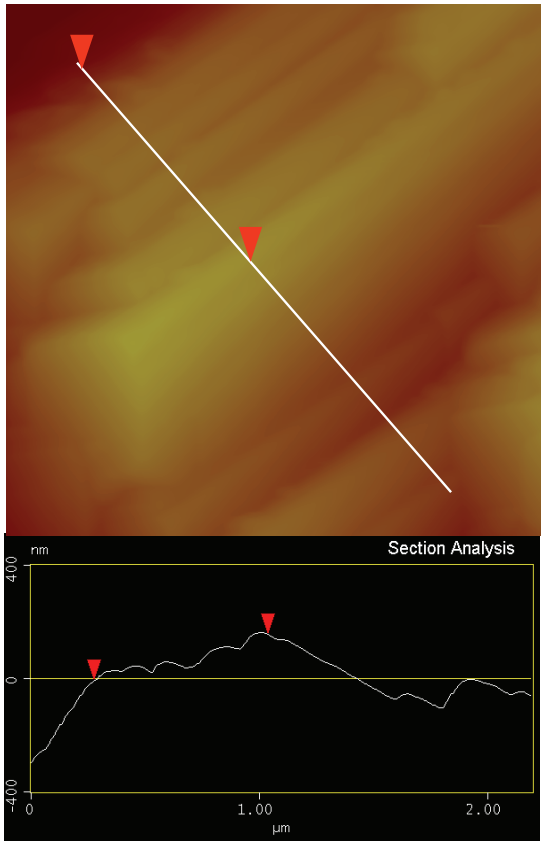

Figure 2: AFM picture and the cross-section analysis of Al40

Figure 3 shows the image of a water drop on a stearic acid passivated Al40 surface. The achieved contact angle for this surface is ~170^o with a contact angle hysteresis (CAH) as low as 4^o. A water drop on a surface with such a low CAH just rolls off even with a fractional inclination angle. For the Al30 surface, on the other hand, where CA is ~150^o with a very high CAH the water drop does not fall from the surface even after tilting the sample to an inclination angle of more than 90^o. The water drop in this case tends to stick to the surface.

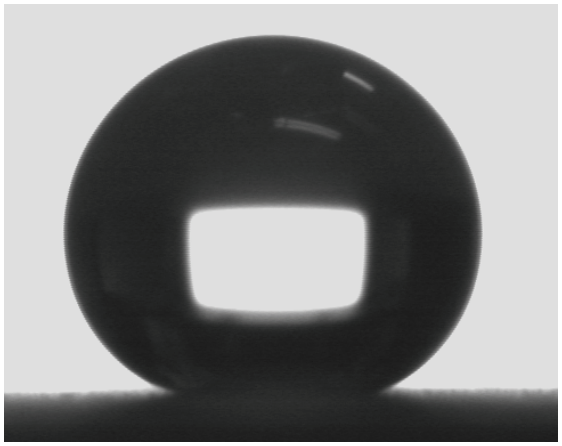

Figure 3: 6 μL water drop of diameter ~ 2.2 mm on the surface of Al40.

The behavior of the CAH with respect to various passivation time of stearic acid has been studied and is shown in Figure 4. The SA Passivation was performed by immersing the samples in the SA solution by varying passivation time between 1 minute and 180 minutes. A large variation in hysteresis value has been observed, while CA remained nearly constant.

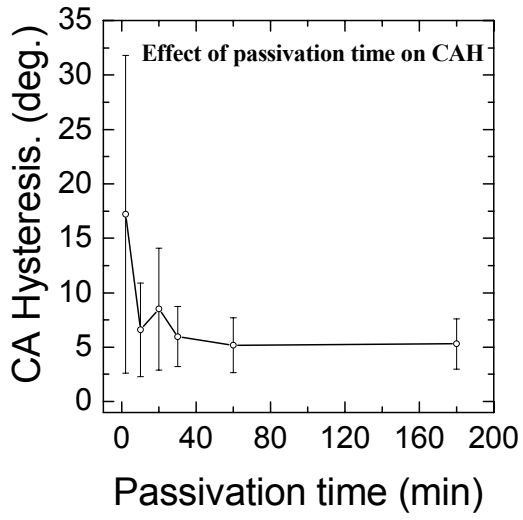

Figure 4: Effect of passivation time on hysteresis of water on sample Al40

A high hysteresis of 15° has been observed after passivation of just one minute. It reduces to nearly 6° after passivating the sample for 10 minutes and water drops already starts rolling off easily. Although a little increase in hysteresis is observed after 20 minutes of passivation, water drops behave the same as with 10 minutes passivated sample. Saturation in hysteresis is observed after 30 minutes of passivation and remains constant even after 180 minutes.

The SA molecules are composed of hydrophilic tails and hydrophobic heads. The hydrophilic tails interact chemically with aluminum/aluminum oxide surfaces. In this passivation process, all the hydrophilic tails become inactive by bonding with the aluminum surface keeping all the hydrophobic heads upward perpendicular to the surface. With such a configuration, the nanostructured aluminum surfaces become highly superhydrophobic. We have used FTIR to understand the presence of SA on SA passivated silicon substrates (as IR does not pass through Al) as shown in Figure 5. The peaks at 2848 and 2917 cm^{-1} were identified as the symmetric and asymmetric vibrations of -CH_2- and -CH_3 groups of the stearic acid, respectively [12].

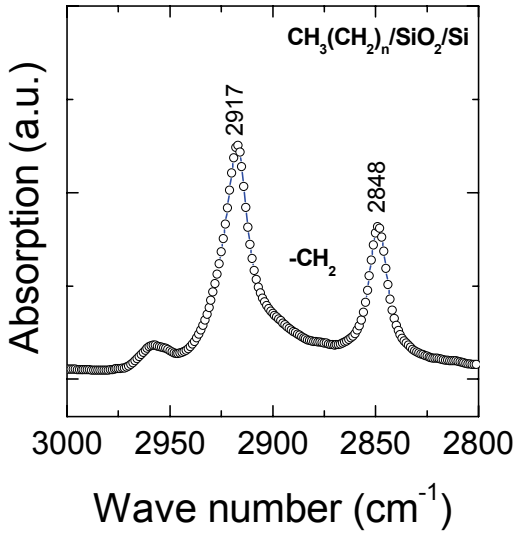

Figure 5: FTIR spectrum of stearic acid on SiO_2/Si surface

The obtained superhydrophobicity of SA passivated aluminum nanostructured surfaces is in agreement with the theory of the Cassie model that explains the behavior of a water drop on a rough composite surface [13]. We have observed that the contact angle of water on a SA passivated smooth silicon surface is only 70°. Achieving a CA of nearly 170° by SA passivation is only possible if the nanostructured pores of the etched surface traps air, whereby the CA of water is 180°. Assuming that the aluminum nanostructured surface is a composite system of

SA and air, a modified Cassie equation can be formulated as follows:

$$\cos\theta_c = f(\cos\theta + 1) - 1 \quad (1)$$

where f is the area fraction of water drop in contact with the surface, θ is the contact angle of SA on a smooth surface and θ_c is the contact angle of the composite system of SA and air. With the obtained contact angles θ_c of 170^o and 150^o for Al40 and Al30 respectively, the corresponding area fraction f is calculated to be 0.011 and 0.099 with the obtained θ value of 70^o for SA on a smooth surface. This difference in area fraction appears pretty distinctly in the FESEM images shown in Figure 1. It is clear from these calculations and observations that the lower the area fraction of water drop in contact with the surface, higher is the superhydrophobicity in a composite system containing a micro-nanostructure.

4 CONCLUSION

Etch pits were created at the dislocation sites of aluminum surfaces by chemical etching. The number of etch pits increases with the increase in concentration of the etchant. FESEM and AFM investigations show that the resulting surface structure is composed of a binary structure of micro and nanosteps similar to the microstructure seen on lotus leaves. These micro-nanopatterned surfaces were passivated using stearic acid organic molecules. The hydrophilic tails of the stearic acid interact with the metal or oxide surfaces keeping their hydrophobic heads upwards normal to the surface. The contact angle of water obtained on such surfaces is as high as 170^o with a hysteresis as low as 4^o. Water drops rolls off these surfaces mimicking the behavior of water drops on lotus leaves. The presence of a binary structure and its passivation with stearic acid molecules produces the lotus effect on aluminum surfaces.

5 ACKNOWLEDGEMENTS

This research was carried out within the framework of the NSERC/Hydro-Quebec/UQAC Industrial Chair on Atmospheric Icing of Power Network Equipment (CIGELE) and Canada Research Chair on Engineering of Power Network Atmospheric Icing (INGIVRE) at Université du Québec à Chicoutimi. The authors would like to thank all the partners of CIGELE/INGIVRE for their financial support. The authors are also thankful to Ms. Hélène Grégoire, of CNRC in Chicoutimi, for providing access to FESEM facilities.

REFERENCES

[1] W. Barthlott, C. Neinhuis, Planta 1, 202, 1997.
[2] Wagner P, F¨urstner R, Barthlott W and Neinhuis C, J. Exp. Bot. 1, 54, 2003.
[3] Lee W, Jin M K, Yoo W C and Lee J K Langmuir 20 7665, 2004.
[4] Gao X and Jiang L, Nature 432, 36, 2004.
[5] R. Blossey, Nature Mater., 2, 301, 2003.
[6] J. Bico, C. Marzolin and D. Quéré, Europhys. Lett., 47, 220, 1999.
[7] K. Tadanaga, N. Katata, T. Minami, J. Am. Ceram. Soc., 80 1040, 1997.
[8] M. Morra, E. Occhiello and F. Garbassi, Langmuir, 5, 872, 1989.
[9] H. Y. Erbil, A. L. Demirel, Y. Avci, O. Mert, Science, 299, 1377, 2003.
[10] N. J. Shirtcliffe, G. McHale, M. I. Newton, and C. C. Perry, Langmuir, 21, 937, 2005.
[11] G. F. Vander Voort, "Metallography: Principles and Practice," McGraw-Hill: New York, 1984
[12] C. R. Kessel, S. Granick, Langmuir, 7, 532, 1991
[13] A. Cassie and S. Baxter, Trans. Faraday Soc., 40, 546, 1944